RESEARCH ARTICLE

The influences of task difficulty and response correctness on neural systems supporting fluid reasoning

M. Layne Kalbfleisch · John W. Van Meter ·
Thomas A. Zeffiro

Abstract This functional magnetic resonance imaging (fMRI) study examined neural contributions to managing task difficulty and response correctness during fluid reasoning. Previous studies investigate reasoning by independently varying visual complexity or task difficulty, or the specific domain. Under natural conditions these factors interact in a complex manner to support dynamic combinations of perceptual and conceptual processes. This study investigated fluid reasoning under circumstances that would represent the cognitive flexibility of real life decision-making. Results from a mixed effects analysis corrected for multiple comparisons indicate involvement of cortical and subcortical areas during fluid reasoning. A 2×2 ANOVA illustrates activity related to variances in task difficulty correlated with increased blood oxygenation level-dependent (BOLD)-signal in the left middle frontal gyrus (BA6). Activity related to response correctness correlated with increased BOLD-signal in a larger, distributed system including right middle frontal gyrus (BA6), right superior parietal lobule (BA7), left inferior parietal lobule (BA40), left lingual gyrus (BA19), and left cerebellum (Lobule VI). The dissociation of function in left BA 6 for task difficulty and right BA6 for response correctness and the involvement of a more diffuse network involving the left cerebellum in response correctness extends knowledge about contributions of classic motor and premotor areas supporting higher level cognition.

Keywords fMRI · Matrix reasoning · Middle frontal gyrus · Brodmann area 6 · Cerebellum · Fluid reasoning · Cognitive flexibility

M. L. Kalbfleisch · J. W. Van Meter · T. A. Zeffiro
Center for Functional and Molecular Imaging, Georgetown University Medical Center, Washington, DC, USA

M. L. Kalbfleisch (✉)
Krasnow Institute for Advanced Study and College of Education and Human Development, George Mason University, 4400 University Drive, MS 2A1, Fairfax, VA 22030, USA
e-mail: mkalbfle@gmu.edu

Introduction

Several neuroimaging experiments have employed adaptations of visual matrix reasoning tests to characterize neural systems related to fluid reasoning in the healthy adult brain (Prabhakaran et al. 1997; Duncan and Owen 2000; Goel et al. 2000; Christoff et al. 2001; Duncan 2001; Kroger et al. 2002; Gray et al. 2003; Geake and Hansen 2005). Fluid reasoning is a type of learning ability. It influences how fast and how much someone learns, including their ability to manipulate and use information in the reasoning process. Matrix tests are composed of series of geometric pictures that are visually incomplete and devoid of linguistic and culturally-based content. Because they lack the language and cultural bias associated with traditional assessments of IQ such as the Wechsler Scales of Intelligence (Wechsler 1939), they are sometimes used to determine general ability or 'g' in lieu of (or in addition to) measuring an IQ score with a traditional assessment. Neuroimaging experiments have demonstrated that matrix tests engage neural systems common to reasoning paradigms grounded in other content domains (Goel et al. 1997, 1998, 2000; Osherson et al. 1998; Goel and Dolan 2001; Prabhakaran et al. 2001;

Luo et al. 2003; Ruff et al. 2003) and from tasks which employ varying reasoning strategies (Rao et al. 1997; Koechlin et al. 1999; Wharton et al. 2000; Goel and Dolan 2003, 2004; van den Heuvel et al. 2003). Therefore, they are an appropriate tool to use in examining neural systems fundamentally associated with the reasoning process.

There is an inherent limitation of fMRI methodology that has lead to an incomplete representation of fluid reasoning in the human brain. Previous reasoning studies are based upon paradigms in which subjects were pre-trained to high performance or expertise for the appropriate purpose of correlating behavioral data with a robust BOLD-contrast signal associated with the subject's behavior in the scanner. While these methods are accepted current practice in the execution of an imaging study, they have lead to an assessment of reasoning as a post-test, testing the brain performing something that it is didactically, in the context of an fMRI experiment, prepared to do, as opposed to demonstrating circumstances more representative of reasoning in real life, such as considering multiple aspects of a problem simultaneously and problem solving under time pressure. It is the difference between characterizing performance on a hard post-test where one draws upon declarative, crystallized knowledge and implicit skill, and an indication of what decision-making looks like ''on the fly,'' a process which supports the demonstration of fluid intelligence.

This study sought to examine fluid reasoning under circumstances that would more accurately portray the cognitive flexibility involved in real life decision-making. To address this in a novel manner, we engaged non-highly trained subjects in a slow event-related fMRI matrix reasoning task in order to assess the BOLD-contrast signal soon after the moment of response. In this design, problem trials varied in their level of difficulty. An additional component of the design imposed a deadline by giving subjects only 20% of the typical time associated with performance on the psychometric version of the matrix reasoning task to solve each problem.

We hypothesized that the neural systems required to perform this reasoning task would include cortical areas related to task type (nonverbal matrix reasoning) and specific regions involved in the decision and response to the problem. In particular, involvement of the following areas was expected: (1) the inferior and medial frontal gyri (BA 9/46, 44, and 47) known to support cognition during abstract problem solving of differing types (deductive, analogical, syllogistic) (Osherson et al. 1998; Goel et al. 2000; Luo et al. 2003); (2) frontal areas that have been shown to support relational complexity and planning (BA 10 and

6) (Christoff et al. 2001; van den Heuvel et al. 2003); and (3) parietal areas (BA 7, 19, and 40) which have been associated with task load and spatial stimulus processing (Prabhakaran et al. 1997; Knauff et al. 2002, 2003; van den Heuvel et al. 2003). Most reasoning studies involving the explicit use of language or implicit semantic verbal strategy generally report stronger left hemispheric activations during reasoning. Some have specifically argued for the role of the left inferior frontal gyrus (BA 44/45/47) in various types of reasoning (Goel et al. 1997, 1998; Knauff et al. 2003; Goel and Dolan 2004). Since the most comprehensive study of the matrix reasoning test, the Raven's Progressive Matrices, or RPM (Raven 1947), reports strong right frontal hemispheric activations for matrix reasoning, in particular, (Prabhakaran et al. 1997), we predicted there would be right frontal hemisphere involvement in this task.

While previous studies have suggested various roles for the frontal cortex during reasoning (i.e. working memory, relational complexity, analogical strategy), specific contributions of the basal ganglia and the cerebellum to the reasoning process have not been explicitly addressed. In particular, a specific role for the cerebellum in higher-level cognition has been a matter of debate. Some submit that efferents from the dentate nucleus in the lateral cerebellum to lateral prefrontal cortex (BA 9/46) via the red nucleus and mediodorsal nucleus of the thalamus play a role in higher level cognition and cognitive flexibility (Leiner et al. 1986; Kim et al. 1994; Middleton and Strick 1994; Schmahmann and Pandya 1995; Karatekin et al. 2000; Molinari et al. 2002; Kelly and Strick 2003). A subset of reasoning studies report activations in the cerebellum but do not suggest a specific explanation for its role in the reasoning process (Rao et al. 1997; Osherson et al. 1998; Goel et al. 2000; Goel and Dolan 2001, 2004; Blackwood et al. 2004). It has been suggested that the cerebellum participates in the process of response reassignment during a complex task (Bischoff-Grethe et al. 2002) or that it supports decision making in uncertain or ambiguous contexts (Blackwood et al. 2004). It has also been shown to play a role in associative learning (Logan and Grafton 1995). This evidence and the constraints utilized in this task to portray conditions representative of real life decision making, that is, solving cognitively difficult problems in a time-dependent manner, led us to hypothesize that the cerebellum would be involved in reasoning under these conditions.

To test these hypotheses, we used a novel non-linguistic ''fluid intelligence'' task in an event-related design and analyzed the fMRI data using a 2×2 analysis of variance (ANOVA) to identify neural

systems associated with the main effects of task difficulty and response correctness, and the interaction between the two variables. This experiment yielded three novel results. First, this experiment demonstrates a statistically robust functional dissociation between the cortical areas subserving task difficulty (L BA6) and response accuaracy (R BA 6). This result qualitatively improves our understanding of how the brain parses out task components in response to psychologically realistic higher cognitive challenges. Second, our results support a functional role for the left cerebellar cortex in encoding response correctness during conditions where the brain receives no external feedback on the accuracy valence of the response. This implies that the brain assesses accuracy based on an internal model and suggests an alternative perspective for exploring higher level cognition. Last, the functional intersection of task difficulty and response correctness demonstrates activation in the subcallosal gyrus (BA 25), an area typically documented in studies designed to assess reward under conditions of uncertainty.

Methods

Subject characterization

Fourteen healthy subjects (9 female, 5 male) determined to be right-handed by the Edinburgh Handedness Inventory with a mean score of 95.7% (range of 80–100) with a mean age of 25.1 years (range 18–47) and mean IQ of 121 (range 101–130) volunteered to participate in this study (see Table 1). All gave written informed consent and were compensated for their participation in accordance with Georgetown University Medical Center and George Mason University IRB approved protocols. Individuals with neurological or medical conditions known to affect brain function or first-degree relatives with neurological, psychiatric, or

Table 1 fMRI adapted-NNAT serial reasoning subject characterization (*n* = 14)

Characteristic	Mean	Range	Correlation
Age	25.1	18–47	
Edinburgh handedness (Right)	95.7	80–100	
Ability measure—WASI–FSIQ	121	101–130	
Ability measure—NNAT–NAI (Level G)	119.4	91–148	FSIQ-NAI 0.58 (*P* < 0.023)
fMRI task—% Hard correct	42.9	14–86	
fMRI Task—% Easy correct	63.1	29–86	

developmental disorders were excluded. Additional exclusion criteria included: current use of psychoactive or vasoactive medications and the consumption of excessive amounts of alcohol, caffeine, or tobacco due to their potential effects on cerebral blood flow (Mulderink et al. 2002).

Behavioral methods

Prior to scanning, subjects were administered the Wechsler Abbreviated Scales of Intelligence (WASI) and Level G of the psychometric version of the Naglieri Nonverbal Ability Test (Naglieri 1997), an untimed nonverbal assessment of general ability that consists of a combination of 38 matrix test items of four reasoning types: serial reasoning, reasoning by analogy, pattern completion, and visual-spatial items. Each subject took approximately 30 min to complete the test. Next, the subjects were briefly introduced to the fMRI task by practicing six sample problems employing NNAT matrix reasoning stimuli that were not used during the fMRI scan.

Task description

The fMRI adapted-NNAT serial reasoning task (NNAT-SRT) is a novel imaging task designed to assess reasoning processes based on 3 × 3 matrix serial reasoning items adapted from the NNAT psychometric instrument. It requires the subject to follow a change across the 3 lines of the matrix problem in order to determine the correct answer in the final iteration of the pattern from five alternative choices provided underneath the matrix (see Fig. 1). Each run consisted of seven easy reasoning problems and seven hard reasoning problems taken from two separate levels of the NNAT, randomized and interleaved with fixation events that varied in duration based on multiples of the 3 s TR (0–12 s). We used a slow event-related design consisting of stimuli presented with variable stimulus onset asynchrony (SOA) generated by OptSeq2 (Greve 2002). The scheduling parameters for this experiment included: 105 time points, a post-stimulus delay window extending from 0 to 24, events of 12 s each, 7 items of each level of the task per run, and 20% null events. This design prevented subjects from anticipating the exact timing of the trials or the problem type within the experimental run. Subjects performed 4 runs presented in counterbalanced order of approximately 5 min in length.

Each reasoning trial consisted of the following sequence: the subject studied the matrix problem for 10 s, followed by a 250 ms tone prompting the subject
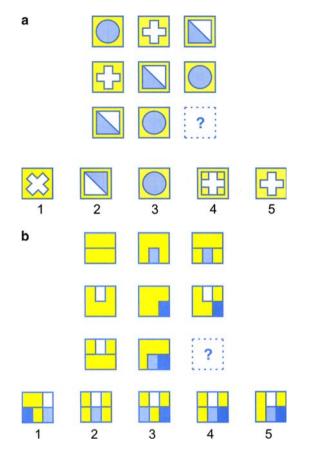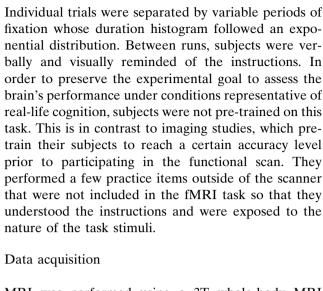
Fig. 1 Sample items from the NNAT-SRT: (**A**) an 'Easy' NNAT Serial Reasoning Item from Level C (correct answer is 5). (**B**) a 'Hard' NNAT Serial Reasoning Item from Level F (correct answer is 4)

to respond. The subject had an additional 1,750 ms to respond for a total trial length of 12 s (see Fig. 2). After the tone, the subject pressed the key on a button box that corresponded to their response using both hands (MRA Inc., Washington, PA). Subjects pressed for answers "1" and "2" with their left hand and answers "3", "4", and "5" with their right hand. Correct answers were counterbalanced within runs.
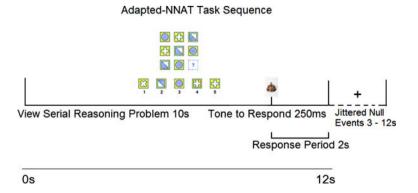
Individual trials were separated by variable periods of fixation whose duration histogram followed an exponential distribution. Between runs, subjects were verbally and visually reminded of the instructions. In order to preserve the experimental goal to assess the brain's performance under conditions representative of real-life cognition, subjects were not pre-trained on this task. This is in contrast to imaging studies, which pre-train their subjects to reach a certain accuracy level prior to participating in the functional scan. They performed a few practice items outside of the scanner that were not included in the fMRI task so that they understood the instructions and were exposed to the nature of the task stimuli.

Data acquisition

MRI was performed using a 3T whole-body MRI scanner (Siemens Magnetom Trio, Erlengen, Germany) and a circularly polarized head coil. Head movement was minimized by padding that was fitted to hold the subject's head in the coil firmly and comfortably. Subjects viewed the stimuli through a mirror mounted on the head coil to reflect the visual stimulus projected onto a screen (209×279 cm) at the back of the bore of the magnet approximately 950 mm from the mirror reflecting the screen. The visual angle subtended by the stimuli was approximately 18°, insuring that the stimuli were presented in subjects' central field of view.

Structural MRI data

Neuroanatomical localization of task-related activity was determined using a structural protocol consisting of three MPRAGE scans acquired during the same scanning session with the following parameters: TR = 1600 ms, TE = 4.38 ms, TI = 640 ms, flip angle 15°, averages = 1, 160 slices with a 1.0 mm thickness, FOV = 256×256 mm^2, effective resolution = $1.0 \times 1.0 \times 1.0^3$ mm, scan time = 6:51 min.

Fig. 2 This diagram depicts the timing and sequence of events in each of the NNAT-SRT trials. Each trial is 12 s in duration

Functional MRI data

Patterns of task-related brain activity were obtained using an echo-planar imaging (EPI) sequence sensitive to BOLD-contrast with the following parameters: TR = 3000 ms, TE = 30 ms, flip angle = 90°, matrix size = 64 × 64, FOV = 192,192 mm^2, 50 slices with a thickness of 2.8 mm and a 0.2 mm gap for an effective resolution of $3.0 \times 3.0 \times 3.0$ mm^3. The first three volumes (9s) of each functional run were discarded to allow for equilibrium in longitudinal magnetization. Four runs each lasting 5.2 min were acquired.

fMRI data analysis

Mixed effects analyses were used to identify the network of regions involved in the task across all levels and regional differences based on task difficulty and correctness of responses. Data analyses were performed using MED × 3.28 (Sensor Systems, Sterling, VA). A first-level analysis was performed on the data from each run of each subject following head motion correction, spatial and temporal filtering, contrast image generation, and spatial normalization to a generalized coordinate space.

Head motion assessment

Head motion was detected using a center of intensity model with an intensity threshold set to 15% of the maximum image intensity. The center of intensity was computed at each time point using all voxels above threshold and then plotted, resulting in a graph depicting the 3D translation of the brain over time. From this estimate of head motion additional metrics were derived. Path length$_{3D}$, a measure that has been used previously to characterize head motion during functional neuroimaging (Eden et al. 1999; Seto et al. 2001), represents the total distance traveled over the course of the whole run in all three dimensions. This provides a measure of total head motion over the course of a run, capturing relatively slow postural adjustments about a stable position. A second measure of head motion, maximum peak-to-peak excursion, was used to assess the absolute distance between the two extremes in head position over the course of the run. This metric captures the extent of gross head motion.

Head motion correction

Head motion was corrected by registering each of the individual time points within the run to the mean of all images in the run using AIR 5.22 (Automated

Table 2 Effectiveness of head motion correction: mean (range)

Measure	Pre	Post
Mean path length 3D (mm)	11.45 (7.36–23.89)	4.92 (3.38–7.26)
Mean maximum peak-to-peak 3D excursion (mm)	0.70 (0.47–1.43)	0.23 (0.14–0.41)

Image Registration, Division of Brain Mapping, UCLA) with a rigid-body model (Woods et al. 1998a, b). Extent of head motion was assessed before and after motion correction. Both path length$_{3D}$ and maximum peak-to-peak excursion were calculated to characterize the degree of head motion (See Table 2).

Filtering

Global variations in intensity across conditions and runs were removed using a ratio normalization procedure dividing the signal in each scan by its mean global signal and scaling the result. Spatially local variations in intensity were corrected using smoothing employing a three-dimensional Gaussian kernel with a FWHM of 6.0 mm (twice the voxel size). Finally, to remove effects related to cardiac and respiratory fluctuations, a high-pass temporal filter was applied with a 128 s period. As the task was presented in an event-related manner the period of the high-pass filter had to be long enough to ensure that no task related signal was removed.

Spatial normalization

The mean EPI image was computed for each run following motion correction and filtering. Transformation from the native EPI space to Talairach space was computed by registering the mean EPI image from each run to the EPI template from SPM99 (Functional Imaging Laboratory, London, UK) using AIR 5.22 with a second-order polynomial warp model with 30 degrees of freedom (Woods et al. 1998b). Differences between ICBM512 space represented by the EPI template and the Talairach atlas were accounted for by converting MNI coordinates to Talairach space using the equations derived by Brett and colleagues (Brett 1999; Duncan et al. 2000).
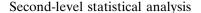
First-level statistical analysis

A multiple regression analysis was used to generate beta-maps and their corresponding Z-maps to examine areas modulated by levels of task difficulty and response correctness. For each subject, four separate reference vectors were constructed: one for each of

the two levels of task difficulty, one for trials corresponding to a correct response, and one for trials corresponding to incorrect responses. For example, the reference vector for the hardest level of task difficulty was coded with a '1' across the entire 12 s during which these trials occurred and a '0' otherwise. Each reference vector was convolved with a Gaussian waveform to model the hemodynamic response expected over the course of the 12 s of a trial. Subjects who either got all of the items in a run wrong (100% incorrect) or correct (100% correct) had to be excluded from the final analysis because the reference vectors corresponding to the inverse correctness would result in a column with all-zeros in the final design matrix, which in turn would result in singular matrix decomposition in the multiple regression analysis.

Quality control

Quality control was performed on each run examining the effectiveness of head motion correction, the quality of activation in the Z-maps from the first-level analysis, and the goodness of the spatial normalization. Each run was assigned an overall score using a Likert scale ranging from 1 to 5 where a score of 5 corresponded to the highest level of quality. A run was assigned a Likert score of 5 if all of the following criteria were met: (1) no activation in ventricles and/or outside the brain, (2) little or no motion related 'ringing' artifacts in the Z-map, (3) a 50% or better reduction in the path length$_{3D}$ head-motion detection metric following motion correction, (4) a post-motion correction maximum peak-to-peak excursion less than 0.25 mm, (5) excellent alignment with the ICBM512 EPI template based on visual inspection of the color overlay of the spatially-normalized mean EPI volume on the template, and (6) evidence of activation in the cortical motor control regions, in particular primary motor cortex bilaterally and the supplementary motor area. Motor cortex activation was used to assess the quality of the Z-maps as activation of these areas were expected irrespective of task difficulty and was unrelated to the reasoning task. The remaining levels of the Likert scores were based on the number of criteria that the run failed to meet. The single functional run with the highest Likert score greater than or equal to 3 out of the four runs that each subject completed was included in the second level analysis. If a subject had two or more runs with the same Likert score, the quality of the behavioral data determined the choice of the run to include in the second level analysis.

Second-level statistical analysis

To meet the requirements of mixed effects analysis, only one run per subject was included at this level based upon the six selection criteria outlined previously in the section on quality control. A 2×2 ANOVA was used to identify the effects of task difficulty and response correctness. Contrasts were created to identify the main-effects of task difficulty and response correctness as well as the interaction of the two. The resulting Z-maps were thresholded at a $P < 0.01$ (uncorrected) with a cluster size of 40 or more voxels. A RESEL correction for multiple comparisons was applied using a whole-brain mask and a corrected P-value threshold of $P < 0.05$ (Worsley et al. 1996).

Results

Psychometric results

The mean score for the psychometric NNAT, the Naglieri Ability Index (NAI), identified general ability in our experimental group (mean 119.4, range 91–148) within 1.6 points of their mean IQ (mean 121, range 101–130) assessed with the Wechsler Abbreviated Scales of Intelligence (WASI) (see Table 1). There was a strong correlation between the Full Scale IQ (FSIQ) measure on the WASI and the Naglieri Ability Index (NAI) on Level G of the psychometric NNAT ($r = 0.58$, $P < 0.023$).

fMRI-adapted NNAT-SRT task performance

Different levels of the task were verified by behavioral performance (see Table 1). The subjects' mean score on Hard trials was 42.9% (14–86) and on Easy trials was 63.1% (29–86).

Head motion

Results of the head motion correction are reported in Table 2. Overall there was 57.1% reduction in mean path length and a reduction in the peak-to-peak excursion to <0.25 mm. The pre-correction mean path length was 11.45 mm, which was reduced to 4.92 mm following motion correction. The mean pre-correction maximum peak-to-peak excursion was 0.70 mm and 0.23 mm following correction. None of the subjects were excluded for head motion.

Table 3 Areas modulated by task difficulty (Hard > Easy) identified from the second-level mixed-effects analysis of the NNAT-SRT

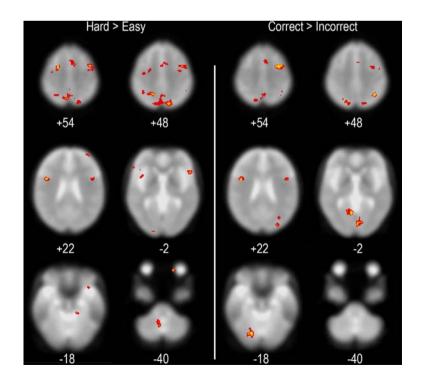| Region Anatomical label	BA	Cluster size (voxels)	Talairach coordinates			Z-score
			x	y	z	
Frontal						
L precentral gyrus	4	47	–38	–11	52	3.26
R medial frontal gyrus	6	106	8	5	52	3.07
L middle frontal gyrus	6	131	–24	1	55	4.28*
R middle frontal gyrus	6	291	28	5	57	3.85
	46	74	42	42	18	3.15
L inferior frontal gyrus	44	119	–46	3	22	3.55
	47	100	–40	13	–5	3.26
R inferior frontal gyrus	47	403	51	14	2	3.43
	47	53	38	19	–12	2.80
Parietal						
R precuneus	7	527	12	–71	48	3.40
L precuneus	7	190	–18	–54	48	3.39
R inferior parietal lobule	40	156	44	–45	40	3.28
Temporal						
R fusiform gyrus	37	90	–38	–33	–11	3.27
Occipital						
R occipital gyrus	19	49	28	–68	28	2.94
L inferior occipital gyrus	18	48	–24	–97	–5	3.01
Cerebellar						
L cerebellum—crus I		72	–36	–79	–27	3.13
L superior posterior—lobule VI		52	–6	–82	–17	2.90
L dentate nucleus		119	–8	–59	–39	3.09

All regions consist of at least 40 voxels with an uncorrected $P < 0.01$ (*significant at $P < 0.05$ following a RESEL correction for multiple comparisons)

Task difficulty

Regions associated with the main effect of difficulty are shown in Table 3. Regions with an uncorrected $P \leq 0.01$ and cluster size threshold of 40 are shown in Fig. 3. Only one area remained significant after a RESEL correction for multiple comparisons: the left middle frontal gyrus (BA 6). There were no significant areas in the Easy > Hard comparison.

Fig. 3 Neuroanatomy of the NNAT-SRT modulated by task difficulty shown on the left (Hard > Easy) and by response correctness (Correct > Incorrect) shown on the right thresholded at a $Z \geq 2.6$ (uncorrected $P < 0.01$) and a cluster size ≥ 20. Images are displayed using the neurological convention with the left hemisphere on the left

Correct versus incorrect trials

After a RESEL correction for multiple comparisons ($P < 0.05$), several areas of the serial reasoning neural system were specific to Correct > Incorrect responses (see Table 4). These include the right medial frontal gyrus (BA6), right superior parietal lobule (BA 7), left inferior parietal lobule (BA 40), the left lingual gyrus (BA 19), and left lobule VI of the cerebellum (see Fig. 3). There were no significant regions identified for incorrect responses greater than correct responses.

Interaction

After a RESEL correction for multiple comparisons ($P < 0.05$), the interaction between the main effects of difficulty and correctness showed one area of significance, the right subcallosal gyrus (BA25) at Talairach coordinates $x = 10$, $y = 15$, $z = -13$.

Table 4 Areas modulated by response correctness Correct > Incorrect identified from the second-level mixed-effects analysis of the NNAT-SRT

Region	BA	Cluster size (voxels)	Talairach coordinates			Z-score
Anatomical label			x	y	z	
Frontal						
R middle frontal gyrus	6	211	27	1	53	4.16*
L inferior frontal gyrus	44	72	–44	3	22	4.03
R precentral gyrus	6	77	53	3	29	3.82
Parietal						
L precuneus	7	82	–2	–68	50	2.92
R precuneus	7	56	10	–77	44	4.03
	7	144	4	–51	59	4.03
R superior parietal lobule	7	71	34	–54	48	4.34*
L inferior parietal lobule	40	273	–28	–60	42	4.06*
Occipital						
R middle occipital gyrus	18	119	30	–85	13	3.77
R lingual gyrus	18	173	2	–81	0	3.85
L lingual gyrus	19	80	–10	–62	–2	4.25*
Cerebellar						
L superior posterior—lobule VI		256	30	–75	–17	4.59*

All regions consist of at least 40 voxels with an uncorrected $P < 0.001$ (*significant at $P < 0.05$ following a RESEL correction for multiple comparisons)

Discussion

This experiment sought to characterize neural systems of fluid reasoning under conditions more closely resembling the cognitive flexibility deployed during real life decision-making. Task difficulty was manipulated by incorporating NNAT reasoning items from various test levels (there are six levels of the NNAT normed by age, and test items become increasingly difficult) to assess the impact of difficulty within the context of ecologically valid matrix reasoning test items. This is in contrast to previous research which administered artificially altered or idiosyncratic stimuli commonly used in studies designed to parse out behavioral performance and neural activation related to perceptual processes such as relational complexity (Christoff et al. 2001; Kroger et al. 2002), or that created artificial stimuli for the purpose of the experiment (Rao et al. 1997). Response correctness was of interest because this condition would indicate the neural system associated with successful, time-dependent decision-making.

Our use of a novel non-linguistic "fluid intelligence" task in a slow event-related design to identify neural systems associated with the reasoning processes and cognitive flexibility required of decision-making in every day life yielded three novel results. Our first result demonstrates a statistically robust functional dissociation between the frontal cortical areas subserving task difficulty (L BA6) and response accuaracy (R BA 6). We propose that this finding sharpens our understanding of how the brain parses out elements of a complex task in response to psychologically realistic higher cognitive challenges. Our second result supports a functional role for the left cerebellar cortex in encoding response correctness during conditions where the brain receives no external feedback on the accuracy of the response. This result suggests that the brain assesses accuracy based on an internal model and provides an alternative perspective for exploring higher level cognition. Lastly, our third result, seen at the functional intersection of task difficulty and response correctness, demonstrates the activation of the subcallosal gyrus (BA 25), an area typically indicated in parametric studies designed to explicitly assess reward and uncertainty.

Neural systems supporting task difficulty and response correctness in fluid reasoning

The primary areas hypothesized to support the reasoning process were verified in these results (see Tables 3 and 4) and include the following areas related to task type (nonverbal matrix reasoning) and specific regions involved in the decision and response to the

problem: the inferior and medial frontal gyri (BA 9/46, 44, and 47) known to support cognition during abstract problem solving of differing types (deductive, analogical, syllogistic) (Osherson et al. 1998; Goel et al. 2000; Luo et al. 2003); (2) frontal areas that have been shown to support relational complexity and planning (BA 10 and 6) (Christoff et al. 2001; van den Heuvel et al. 2003); and (3) parietal areas (BA 7, 19, and 40) which are associated with task load and spatial stimulus processing (Prabhakaran et al. 1997; Knauff et al. 2002, 2003; van den Heuvel et al. 2003). Most reasoning studies involving the explicit use of language or implicit semantic verbal strategy generally report stronger left hemispheric activations during reasoning. Some have specifically argued for the role of the left inferior frontal gyrus (BA 44/45/47) in various types of reasoning (Goel et al. 1997, 1998; Knauff et al. 2003; Goel and Dolan 2004). Since the most comprehensive study of the matrix reasoning test, the Raven's Progressive Matrices, or RPM (Raven 1947), reports strong right frontal hemispheric activations for matrix reasoning, in particular, (Prabhakaran et al. 1997), we predicted there would be right frontal hemisphere involvement in this task.

More specifically, the pattern of frontal cortex activation in the main effects of difficulty and correctness dissociates the roles of the left middle frontal gyrus (lateral BA 6) and the right middle frontal gyrus (lateral BA 6) respectively during fluid reasoning. Under these conditions, we speculate that this area of the lateral frontal cortex is differentially recruited to facilitate two distinct aspects of cognitive processing in fluid reasoning. The role of Brodmann's area 6 in higher level cognition has been investigated in relationship to working memory (Smith and Jonides 1999; Owen et al. 2005), and associated with reasoning on tasks based on arbitrary content (Goel and Dolan 2003). One study which examined the role of the middle frontal gyrus (BA 6) during a cognitive task using TMS and fMRI reports that the medial portion of this gyrus updates verbal information in working memory during cognitive processing while the lateral portion of this gyrus is responsible for updating spatial information (Tanaka et al. 2005). The experiment from the study by Tanaka and colleagues was based on a mental operations task, which required the sequential update of verbal or spatial representations in memory. The spatial stimuli in their task were the indication of a marker in one of nine slots on a square grid. This detail is important because their spatial stimuli could be visually and heuristically compared to the 3×3 serial matrices in our task. The coordinates they identify in their experiment for lateral frontal cortex (L: –25, 3, 56;

R: 23, 4, 56) are nearly identical to the coordinates reported in our study in association with task difficulty (L: –24, 1, 55) and response correctness (R: 27, 1, 53). A reasoning experiment on three-term relational reasoning by Goel and Dolan (2001) involving concrete versus abstract stimuli in both verbal and spatial domains also report coordinates for bilateral middle frontal gyri (BA 6) almost identical to ours in their main effect (L: –27, 3, 51; R: 30, 9, 51) but do not distinguish contributions from the left and right hemispheres.

Three experiments designed to understand the roles of the lateral frontal cortex (BA 6) versus the posterior parietal cortex in working memory, one using ERPs (Vogel and Machizawa 2004), and the others using fMRI (Todd and Marois 2004; Owen 2004) provide evidence that the posterior parietal cortex stores representations of visual information while the contributions of the lateral frontal cortex perform top–down executive processes on those stored representations (Owen 2004). In light of these studies and the results reported here, it appears that the this area of the lateral frontal cortex (BA 6) subserves at least two functions during reasoning on this task, one typically associated with updating or manipulating spatial information being held by the posterior parietal cortex (mainly in precuneate—BA 7 and inferior parietal cortex—BA 40), and another that relates to encoding the status of that information (providing a correct solution to the problem). Within the context of this study, the left lateral cortex (BA 6) is supporting processing related to the difficulty or complexity of the problem. Though this area is the only area in the neural system that survives correction for multiple comparisons, there is a greater network that includes efferents comprising a cerebrocerebellar pathway projecting from the dentate nucleus, through the thalamus, to BA 46, the area of the dorsolateral prefrontal cortex classically associated with working memory in the prefrontal cortex. We suggest that this network was not more strongly detected because the assignment of Hard and Easy items came directly from different levels of the psychometric NNAT and were not artificially altered to parametrically probe difficulty in the manner of classically designed studies of working memory load and therefore, were not as distinct.
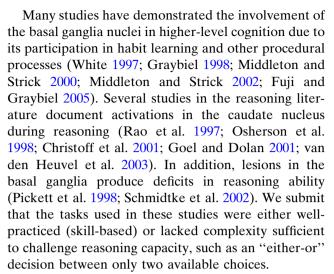
Role of the cerebellum in response correctness

The extant literature has suggested that the cerebellum assists in cognitive tasks that are difficult to solve (Kim et al. 1994), involve hypothesis generation or a self-determined solution (Fiez 1996; Elliott et al. 1997),

require planning (Fiez et al. 1992; Grafman et al. 1992; Karatekin et al. 2000) and inferential processes to solve problems (Goel et al. 2000), or which occur in contexts of uncertainty (Blackwood et al. 2004). The activation of the left cerebellum in our results is consistent with other studies indicating its role in cognitive processing (Allen et al. 1997; Van Mier et al. 1998; Blackwood et al. 2004). Previous work has shown that the left cerebellum is active during attention tasks that have no motor requirements while the right is active during tasks which have motor but no cognitive requirements (Allen et al. 1997) and that the left cerebellum, in particular, is more strongly involved in cognitive versus motor tasks (Van Mier et al. 1998; Van Mier and Petersen 2002). This finding also supports the activation of right middle frontal gyrus (BA 6) during response correctness, as it receives projections originating in the contralateral cerebellum (Schmahmann and Pandya 1997a,b). If the cerebellar activations found in our study were only related to a motor response, then bilateral activations would have been present as both hands were used in the subject's response (responses 1 and 2 were given with the left hand and 3–5 were given with the right).

Solving the reasoning problems in this task required the subject to evaluate the matrix and the possible five answers provided in the trial to determine the correct response. A previous study demonstrated that in addition to coordinating a motor response, the cerebellum facilitates the re-assignment of a response when there are multiple alternatives available (Bischoff-Grethe et al. 2002). Studies that report cerebellar involvement in their tasks instead of, or in addition to, the basal ganglion, utilize tasks that require subjects to monitor complex changes beyond a compare and contrast decision, a single change in relational complexity, or other property of the stimulus (Rao et al. 1997; Goel et al. 2000; Goel and Dolan 2001). Positron emission tomography (PET) studies of serial reaction time testing demonstrate cerebellar involvement during the learning phase of testing and associate its involvement with implicit learning and sequence detection (Jenkins et al. 1994) and associative learning (Logan and Grafton 1995). Further, patients with cerebellar lesions and other disorders affecting the cerebellum (Schmahmann 2004) suffer visual-spatial deficits and have difficulty with sequence learning (Petrosini et al. 1998; Nixon and Passingham 2000; Molinari et al. 2004), planning (Grafman et al. 1992), and impaired eyeblink conditioning in the absence of motor deficits (Solomon et al. 1989; Daum et al. 1993; Topka et al. 1993).

Many studies have demonstrated the involvement of the basal ganglia nuclei in higher-level cognition due to its participation in habit learning and other procedural processes (White 1997; Graybiel 1998; Middleton and Strick 2000; Middleton and Strick 2002; Fuji and Graybiel 2005). Several studies in the reasoning literature document activations in the caudate nucleus during reasoning (Rao et al. 1997; Osherson et al. 1998; Christoff et al. 2001; Goel and Dolan 2001; van den Heuvel et al. 2003). In addition, lesions in the basal ganglia produce deficits in reasoning ability (Pickett et al. 1998; Schmidtke et al. 2002). We submit that the tasks used in these studies were either well-practiced (skill-based) or lacked complexity sufficient to challenge reasoning capacity, such as an "either-or" decision between only two available choices.

When the NNAT is administered psychometrically, each item typically requires 30–60 s to solve correctly. However, the modified version of the task used during scanning limited the subjects to only 12 s per item in order to mimic real life constraints on decision-making. Perceptual attention tasks have been shown to recruit the cerebellum bilaterally in comparisons based on the speed of presentation, with activity in the cerebellum associated with high speed presentation (low speed versus high speed) (Lazeron et al. 2003). Evidence from PET and transcranial magnetic stimulation (TMS) studies that argue cerebellar and motor cortex activations are characteristic of implicit stages of visuo-motor skill learning and that these activations decrease when the skill becomes explicit (Pascual-Leone et al. 1994; Doyon et al. 1996; Petersen et al. 1998). Thus, it is possible that the speed of the trials, along with the novelty of the test items, created conditions requiring the cognitive flexibility that has been associated with the recruitment of the cerebellum (Leiner et al. 1986; Kim et al. 1994; Middleton and Strick 1994; Schmahmann and Pandya 1995; Karatekin et al. 2000; Molinari et al. 2002; Kelly and Strick 2003).

What is the potential significance of the cerebellum in this task and how may we characterize the involvement of the cerebellum in reasoning? A review of the possible different roles of the cerebellum and parietal cortex in sensorimotor action prediction suggests that the cerebellum may be a part of a response mechanism that functions on a level of sensory unawareness (Blakemore and Sirigu 2003). In other words, in the context of models such as the 'forward dynamic' and 'forward output' models suggested by Miall and colleagues, which make predictions about the behavior of the motor system (Miall et al. 1993; Wolpert et al. 1995), the cerebellum may aid early perceptual

processing about the facilitatory motor response apart from the parietal cortex. In the context of the time-dependent reasoning required during this experiment, one could argue that the cerebellum, playing a role in action prediction and in the diffuse but anatomically coherent neural system shown to support response correctness, contributes a particular neural emphasis during successful problem solving. It is providing internal guidance to the brain in the absence of explicit external feedback about performance.

In the main effect of response correctness, the left superior posterior cerebellum is significant after correction for multiple comparisons as well as the left inferior parietal lobule (BA 40) and the right superior parietal lobule (BA 7). Perhaps, this anatomical cerebellar-parietal distinction between sensory unaware prediction and sensory integration and planning is guiding cognition during a successful trial. The brain's distinct functional signature associated with response correctness in the absence of external feedback lends support for the idea of 'mental dexterity' underwritten by the cerebellum during higher level cognition (Leiner et al. 1986).

Assessing fluid reasoning

Participants in this study were not pre-trained to reach a certain level of task performance. This was to aid the ability to capture neural processes associated with decision-making under novel and time-dependent conditions as subjects were given only 12 s to complete each trial. Despite this, several measures were taken to preserve the validity of our statistical results. First, problem trials were jittered in time to prevent subjects from anticipating the onset of a trial and to enable our ability to correlate the behavioral response with the BOLD-contrast signal. Second, the behavioral data verifies two levels of difficulty (Hard and Easy) with performance proficiencies at 63.1% for Easy items and 42.9% for Hard items (see Table 1). While these performance percentages are lower than typical standards of behavioral performance correlated with neural activation on an fMRI task, they are still well above the chance level (20%) for this task. Unfortunately, runs that included a performance of 100% accuracy on either or both of the Hard and Easy trial items were unable to be included in the analysis because this condition created a singular matrix problem with the analysis software. Third, we elaborate our techniques and results for quality control and head motion detection and correction in order to demonstrate that the signal intensities reported here are not resulting from

artifact, but correspond to the behavioral response on this task. Finally, we employed a conservative, mixed effects analysis on these data, requiring the use of only one observation (one run) per subject, and performed an ANOVA correcting for multiple comparisons using a RESEL correction at $P < 0.05$.

Our third result, the activation of the subcallosal gyrus (BA 25), found for the interaction between the effects of difficulty and correctness, was not an area that we predicted in our hypothesis. However, several imaging experiments suggest the subcallosal gyrus is involved in decision-making and reinforcement under conditions of uncertainty (Elliott et al. 1997; Kilts et al. 2001; Paulus et al. 2002; Rogers et al. 2004). Given the difficulty of the task (see behavioral performance means in Table 1) and the absence of external feedback during the task, uncertainty about performance may have contributed to the recruitment of this area. This is an exciting result, as it hints at an intersection between cognitive and limbic processes in the orbitofrontal cortex that are not currently well understood in the context of higher level cognition. Results of a study examining the neural basis of strategy interference during reasoning detected areas of the orbital frontal cortex in association with the presence of cognitive conflict (Stavy et al. 2006). The coordinates of these areas are not similar to the ones detected in our experiment, which suggests a role for this "prelimbic" area in assessing risk and reward during naturalistic reasoning conditions.

Conclusion

This study sought to examine neural systems of problem solving supporting fluid reasoning in a less constrained manner in order to more accurately portray systems associated with cognitive flexibility and decision-making in real life. This was achieved by administering completely novel matrix reasoning items in the scanner with a stringent deadline for problem solving embedded in a slow event-related design so that subjects would be unable to exhibit a training effect. Examining the influences of task difficulty and response correctness on time-dependent fluid reasoning provides new evidence of the relative contributions of a diffuse but anatomically coherent network, the cerebrocerebellar system, to decision-making. Analysis of the main effects of task difficulty and response correctness demonstrate a dissociation of function in lateral frontal cortex between solving and responding to a problem correctly (R middle frontal gyrus, BA 6) versus managing the difficulty of a problem (L middle frontal

gyrus, BA 6), lending new insight into the functional specialization of BA 6 in higher level cognition. Brodmann's area 6 appears to perform executive functions on information held in posterior parietal cortices (BA 7 and 40) with the left BA 6 supporting encoding related to task difficulty and the right BA 6 supporting accurate decision-making under time-dependent conditions. Further inspection of the neural systems identified in this task support the role of the cerebellum and the larger pathways comprising the cerebrocerebellar system in fluid reasoning. We submit that the subcortical support for frontal systems during reasoning depends not only on the complexity of the content of the task stimuli but also on whether or not practiced skill is being exercised and the context of the problem trial.

From an evolutionary perspective, the cerebellum has been shown to support basic functions including movement and attention. As such, it represents a neural mechanism that may not only assist rapid environmental assessment but also support complex cognitive problem solving. It has been suggested that human intelligence may result not so much from qualitative differences in our cortex but from a combination and enhancement of abilities (Roth and Dicke 2005). The representation of the cerebrocerebellar system and the subcallosal gyrus in novel and time-dependent fluid reasoning suggests that there are broader representations of higher level cognition than are currently documented or well understood. Future studies are required to continue to parse out how context affects neural systems associated with fluid reasoning, how neural systems of cognition and reward interact and facilitate problem solving under conditions of uncertainty, and the specific contributions of the motor system to higher level cognition.

References

Allen G, Buxton RB, Wong EC, Courchesne E (1997) Attentional activation of the cerebellum independent of motor involvement. Science 275:1940–1943

Bischoff-Grethe A, Ivry RB, Grafton ST (2002) Cerebellar involvement in response reassignment rather than attention. J Neurosci 22:546–553

Blackwood N, Ffytche D, Simmons A, Bentall R, Murray R, Howard R (2004) The cerebellum and decision making under uncertainty. Brain Res Cogn Brain Res 20:46–53

Blakemore SJ, Sirigu A (2003) Action prediction in the cerebellum and in the parietal lobe. Exp Brain Res 153:239–245

Brett M (1999) The MNI Brain and the Talairach Atlas

Christoff K, Prabhakaran V, Dorfman J, Zhao Z, Kroger JK, Holyoak KJ, Gabrieli JD (2001) Rostrolateral prefrontal cortex involvement in relational integration during reasoning. NeuroImage 14:1136–1149

Daum I, Schugens MM, Ackermann H, Lutzenberger W, Dichgans J, Birbaumer N (1993) Classical conditioning after cerebellar lesions in humans. Behav Neurosci 107:748–756

Doyon J, Owen AM, Petrides M, Sziklas V, Evans AC (1996) Functional anatomy of visuomotor skill learning in human subjects examined with positron emission tomography. Eur J Neurosci 8:637–648

Duncan J (2001) An adaptive coding model of neural function in prefrontal cortex. Nat Rev Neurosci 2:820–829

Duncan J, Owen AM (2000) Common regions of the human frontal lobe recruited by diverse cognitive demands. Trends Neurosci 23:475–483

Duncan J, Seltz RJ, Kolodny J, Bor D, Herzog H, Ahmed A, Newell FN, Emslie H (2000) A neural basis for general intelligence. Am J Ophthalmol 130:687

Eden GF, Joseph JE, Brown HE, Brown CP, Zeffiro TA (1999) Utilizing hemodynamic delay and dispersion to detect fMRI signal change without auditory interference: the behavior interleaved gradients technique. Magn Reson Med 41:13–20

Elliott R, Frith CD, Dolan RJ (1997) Differential neural response to positive and negative feedback in planning and guessing tasks. Neuropsychologia 35:1395–1404

Fiez JA (1996) Cerebellar contributions to cognition. Neuron 16:13–15

Fiez JA, Petersen SE, Cheney MK, Raichle ME (1992) Impaired non-motor learning and error detection associated with cerebellar damage: a single case study. Brain 115 Pt 1:155–178

Fuji N, Graybiel AM (2005) Time-varying covariance of neural activities recorded in striatum and frontal cortex as monkeys perform sequential-saccade tasks. Proc Natl Acad Sci 102(25):9032–9037

Geake JG, Hansen PC (2005) Neural correlates of intelligence as revealed by fMRI of fluid analogies. NeuroImage 26(2):555–564

Goel V, Buchel C, Frith C, Dolan RJ (2000) Dissociation of mechanisms underlying syllogistic reasoning. NeuroImage 12:504–514

Goel V, Dolan RJ (2001) Functional neuroanatomy of three-term relational reasoning. Neuropsychologia 39:901–909

Goel V, Dolan RJ (2003) Reciprocal neural response within lateral and ventral medial prefrontal cortex during hot and cold reasoning. NeuroImage 20:2314–2321

Goel V, Dolan RJ (2004) Differential involvement of left prefrontal cortex in inductive and deductive reasoning. Cognition 93:B109–121

Goel V, Gold B, Kapur S, Houle S (1997) The seats of reason? An imaging study of deductive and inductive reasoning. Neuroreport 8:1305–1310

Goel V, Gold B, Kapur S, Houle S (1998) Neuroanatomical correlates of human reasoning. J Cogn Neurosci 10:293–302

Grafman J, Litvan I, Massaquoi S, Stewart M, Sirigu A, Hallett M (1992) Cognitive planning deficit in patients with cerebellar atrophy. Neurology 42:1493–1496

Gray JR, Chabris CF, Braver TS (2003) Neural mechanisms of general fluid intelligence. Nat Neurosci 6:316–322

Graybiel AM (1998) The basal ganglia and chunking action repertoires. Neurobiol Learn Memory 70(1–2):119–136

Jenkins IH, Brooks DJ, Nixon PD, Frackowiak RS, Passingham RE (1994) Motor sequence learning: a study with positron emission tomography. J Neurosci 14:3775–3790

Karatekin C, Lazareff JA, Asarnow RF (2000) Relevance of the cerebellar hemispheres for executive functions. Pediatr Neurol 22:106–112

Kelly RM, Strick PL (2003) Cerebellar loops with motor cortex and prefrontal cortex of a nonhuman primate. J Neurosci 23:8432–8444

Kilts CD, Schweitzer JB, Quinn CK, Gross RE, Faber TL, Muhammad F, Ely TD, Hoffman JM, Drexler KP (2001) Neural activity related to drug craving in cocaine addiction. Arch Gen Psychiatry 58:334–341

Kim SG, Ugurbil K, Strick PL (1994) Activation of a cerebellar output nucleus during cognitive processing. Science 265:949–951

Knauff M, Fangmeier T, Ruff CC, Johnson-Laird PN (2003) Reasoning models and images: behavioral measures and cortical activity. J Cogn Neurosci 15:559–573

Knauff M, Mulack T, Kassubek J, Salih HR, Greenlee MW (2002) Spatial imagery in deductive reasoning: a functional MRI study. Brain Res Cogn Brain Res 13:203–212

Koechlin E, Basso G, Pietrini P, Panzer S, Grafman J (1999) The role of the anterior prefrontal cortex in human cognition. Nature 399:148–151

Kroger JK, Sabb FW, Fales CL, Bookheimer SY, Cohen MS, Holyoak KJ (2002) Recruitment of anterior dorsolateral prefrontal cortex in human reasoning: a parametric study of relational complexity. Cereb Cortex 12:477–485

Lazeron RH, Rombouts SA, de Sonneville L, Barkhof F, Scheltens P (2003) A paced visual serial addition test for fMRI. J Neurol Sci 213:29–34

Leiner HC, Leiner AL, Dow RS (1986) Does the cerebellum contribute to mental skills?. Behav Neurosci 100:443–454

Logan CG, Grafton ST (1995) Functional anatomy of human eyeblink conditioning determined with regional cerebral glucose metabolism and positron-emission tomography. Proc Natl Acad Sci 92(16):7500–7504

Luo Q, Perry C, Peng D, Jin Z, Xu D, Ding G, Xu S (2003) The neural substrate of analogical reasoning: an fMRI study. Brain Res Cogn Brain Res 17:527–534

Miall RC, Weir DJ, Wolpert DM, Stein JF (1993) Is the cerebellum a smith predictor? J Motor Behav 25(3):203–216

Middleton FA, Strick PL (1994) Anatomical evidence for cerebellar and basal ganglia involvement in higher cognitive function. Science 266:458–461

Middleton FA, Strick PL (2000) Basal ganglia and cerebellar loops: motor and cognitive circuits. Brain Res Brain Res Rev 31:236–250

Middleton FA, Strick PL (2002) Basal-ganglia 'projections' to the prefrontal cortex of the primate. Cerebral Cortex 12:926–935

Molinari M, Filippini V, Leggio MG (2002) Neuronal plasticity of interrelated cerebellar and cortical networks. Neuroscience 111:863–870

Molinari M, Petrosini L, Misciagna S, Leggio MG (2004) Visuospatial abilities in cerebellar disorders. J Neurol Neursurg Psychiatry 75:235–240

Mulderink TA, Gitelman DR, Mesulam MM, Parrish TB (2002) On the use of caffeine as a contrast booster for BOLD fMRI studies. NeuroImage 15:37–44

Naglieri J (1997) The Naglieri nonverbal ability test. Psychological Corporation, San Antonio

Nixon PD, Passingham RE (2000) The cerebellum and cognition: cerebellar lesions impair sequence learning but not conditional visuomotor learning in monkeys. Neuropsychologia 38:1054–1072

Osherson D, Perani D, Cappa S, Schnur T, Grassi F, Fazio F (1998) Distinct brain loci in deductive versus probabilistic reasoning. Neuropsychologia 36:369–376

Owen AM (2004) Working memory: imaging the magic number four. Curr Biol 14:573–574

Owen AM, McMillan KM, Laird AR, Bullmore E (2005) N-back working memory paradigm: a meta-analysis of normative functional neuroimaging studies. Human Brain Mapping 25:46–59

Pascual-Leone A, Grafman J, Hallett M (1994) Modulation of cortical motor output maps during development of implicit and explicit knowledge. Science 263:1287–1289

Paulus MP, Hozack N, Frank L, Brown GG (2002). Error rate and outcome predictability affect neural activation in prefrontal cortex and anterior cingulate during decision-making. Neuroimage 15(4):836–846

Petersen SE, van Mier H, Fiez JA, Raichle ME (1998) The effects of practice on the functional anatomy of task performance. PNAS 95:853–860

Petrosini L, Leggio MG, Molinari M (1998) The cerebellum in the spatial problem solving: a co-star or a guest star? Prog Neurobiol 56:191–210

Pickett ER, Kuniholm E, Protopapas A, Friedman J, Lieberman P (1998) Selective speech motor syntax and cognitive deficits associated with bilateral damage to the putamen and the head of the caudate nucleus: a case study. Neuropsychologia 36:173–188

Prabhakaran V, Rypma B, Gabrieli JD (2001) Neural substrates of mathematical reasoning: a functional magnetic resonance imaging study of neocortical activation during performance of the necessary arithmetic operations test. Neuropsychology 15:115–127

Prabhakaran V, Smith JA, Desmond JE, Glover GH, Gabrieli JD (1997) Neural substrates of fluid reasoning: an fMRI study of neocortical activation during performance of the Raven's Progressive Matrices Test. Cogn Psychol 33:43–63

Raven JC (1947) Raven's progressive matrices. Psychological Corporation, San Antonio

Rao SM, Bobholz JA, Hammeke TA, Rosen AC, Woodley SJ, Cunningham JM, Cox RW, Stein EA, Binder JR (1997) Functional MRI evidence for subcortical participation in conceptual reasoning skills. Neuroreport 8:1987–1993

Rogers RD, Ramnani N, Mackay C, Wilson JL, Jezzard P, Carter CS, Smith SM (2004) Distinct portions of anterior cingulate cortex and medial prefrontal cortex are activated by reward processing in separable phases of decision-making cognition. Biol Psychiatry 55:594–602

Roth G, Dicke U (2005) Evolution of the brain and intelligence. Trends Cogn Sci 9:250–257

Ruff CC, Knauff M, Fangmeier T, Spreer J (2003) Reasoning and working memory: common and distinct neuronal processes. Neuropsychologia 41:1241–1253

Schmahmann JD (2004) Disorders of the cerebellum: ataxia dysmetria of thought and the cerebellar cognitive affective syndrome. J Neuropsychiatry Clin Neurosci 16:367–378

Schmahmann JD, Pandya DN (1995) Prefrontal cortex projections to the basilar pons in rhesus monkey: implications for the cerebellar contribution to higher function. Neurosci Lett 199:175–178

Schmahmann JD, Pandya DN (1997a) Anatomic organization of the basilar pontine projections from prefrontal cortices in rhesus monkey. J Neurosci 17:438–458

Schmahmann JD, Pandya DN (1997b) The cerebrocerebellar system. Int Rev Neurobiol 41:31–60

Schmidtke K, Manner H, Kaufmann R, Schmolck H (2002) Cognitive procedural learning in patients with fronto-striatal lesions. Learn Mem 9:419–429

Seto E, Sela G, McIlroy WE, Black SE, Staines WR, Bronskill MJ, McIntosh AR, Graham SJ (2001) Quantifying head motion associated with motor tasks used in fMRI. NeuroImage 14:284–297

Smith EE, Jonides J (1999) Storage and executive processes in the frontal lobes. Science 283:1657–1661

Solomon PR, Stowe GT, Pendlebury WW (1989) Disrupted eyelid conditioning in a patient with damage to cerebellar afferents. Behav Neurosci 103:898–902

Stavy R, Goel V, Critchley H, Dolan R (2006) Intuitive interference in quantitative reasoning. Brain Res 1073–1074:383–388

Tanaka S, Honda M, Sadato N (2005) Modality-specific cognitive function of medial and lateral human brodmann area 6. J Neurosci 25:496–501

Todd JJ, Marois R (2004) Capacity limit of visual short term memory in human posterior parietal cortex. Nature 428:751–754

Topka H, Valls Sole J, Massaquoi SG, Hallett M (1993) Deficit in classical conditioning in patients with cerebellar degeneration. Brain 116:961–969

Van den Heuvel OA, Groenewegen HJ, Barkhof F, Lazeron RH, van Dyck R, Veltman DJ (2003) Frontostriatal system in planning complexity: a parametric functional magnetic resonance version of Tower of London task. NeuroImage 18:367–374

Van Mier HI, Tempel LW, Perlmutter JS, Raichle ME, Petersen SE (1998) Changes in brain activity during motor learning measured with PET: effects of hand of performance and practice. J Neurophysiol 80:2177–2199

Van Mier HI, Petersen SE (2002) Role of the cerebellum in motor cognition. Ann NY Acad Sci 978:334–353

Vogel EK, Machizawa MG (2004) Neural activity predicts individual differences in visual working memory capacity. Nature 428:748–751

Wechsler D (1939) The measurement of adult intelligence. Williams and Wilkins Company, Baltimore

Wharton CM, Grafman J, Flitman SS, Hansen EK, Brauner J, Marks A, Honda M (2000) Toward neuroanatomical models of analogy: a positron emission tomography study of analogical mapping. Cogn Psychol 40:173–197

White NM (1997) Mnemonic functions of the basal ganglia. Curr Opin Neurobiol 7:164–169

Wolpert DM, Ghahramani Z, Jordan MI (1995) An internal model for sensorimotor integration. Science 269:1880–1882

Woods RP, Grafton ST, Holmes CJ, Cherry SR, Mazziotta JC (1998a) Automated image registration: I General methods and intrasubject intramodality validation. J Comput Assist Tomo 22:139–152

Woods RP, Grafton ST, Watson JD, Sicotte NL, Mazziotta JC (1998b) Automated image registration: II Intersubject validation of linear and nonlinear models. J Comput Assist Tomog 22: 53–165

Worsley KJ, Marrett S, Neelin P, Vandal AC, Friston KJ, Evans AC (1996) A unified statistical approach for determining significant signals in images of cerebral activation. Human Brain Mapping 4:58–73